Sequential motif profiles and topological plots for offline signature verification

Elias N. Zois and Evangelos Zervas
University of West Attica
Ancient olive grove campus, 12241, Greece
{ezois, ezervas}@uniwa.gr

Dimitrios Tsourounis and George Economou
University of Patras
Patras, 26500, Greece
{dtsourounis, economou}@upatras.gr

Abstract

In spite of the overwhelming high-tech marvels and applications that rule our digital lives, the use of the handwritten signature is still recognized worldwide in government, personal and legal entities to be the most important behavioral biometric trait. A number of notable research approaches provide advanced results up to a certain point which allow us to assert with confidence that the performance attained by signature verification (SV) systems is comparable to those provided by any other biometric modality. Up to now, the mainstream trend for offline SV is shared between standard -or handcrafted- feature extraction methods and popular machine learning techniques, with typical examples ranging from sparse representation to Deep Learning. Recent progress in graph mining algorithms provide us with the prospect to re-evaluate the opportunity of utilizing graph representations by exploring corresponding graph features for offline SV. In this paper, inspired by the recent use of image visibility graphs for mapping images into networks, we introduce for the first time in offline SV literature their use as a parameter free, agnostic representation for exploring global as well as local information. Global properties of the sparsely located content of the shape of the signature image are encoded with topological information of the whole graph. In addition, local pixel patches are encoded by sequential visibility motifs-subgraphs of size four, to a low six dimensional motif profile vector. A number of pooling functions operate on the motif codes in a spatial pyramid context in order to create the final feature vector. The effectiveness of the proposed method is evaluated with the use of two popular datasets. The local visibility graph features are considered to be highly informative for SV; this is sustained by the corresponding results which are at least comparable with other classic state-of-the-art approaches.

1. Introduction

Despite the advancement and growth in several biometric modalities, the handwritten signature remains a very popular way for a person to declare his/her consent or attendance throughout a governmental, personal or financial action [1-2], with imminent applications to a non-invasive, friendly and secure environment for security oriented e-society applications [3]. Signatures are characterized as a behavioral biometric; they are usually acquired and stored with the help of low cost sensors (e.g. mobile phones, PDA's, etc.) that records the outcome of the executed personal signing process. According to the type of sensor, signatures can be acquired either in a dynamic mode (or online) [4-7] or in a static mode (or offline). The offline SV usually considers grayscale images as input to an assembly of computer vision and pattern recognition (CVPR) algorithms in order to carry out the task of authenticating an individual, by means of his/hers signature. During the last forty years, signature verification (SV), defined as the act or art of verifying the presence of an individual by means of his signature, has gained considerable attention from the scientific community. This is easily supported by a considerable number of comprehensive surveys and state-of-the-art reviews in automatic SV (ASV) [8-13] that have been published up to now.

A set of handwritten signatures performed by the same person are by definition diverse; that is, no two signatures are ever the same [14]. This intrapersonal variation affects any mapping procedure from the image domain to the representation or feature space. Ideally, any signature mapping must preserve any valuable intrapersonal information, which is vital to the verification stage that follows. During the preceding decade, the mainstream research effort in offline signature representation was dominated by the use of classical or handcrafted computer vision feature vectors. A taxonomy on these methods distinguishes feature extraction by leveraging global and/or local methods. Global information methods explore among others geometric features like signature height, width, area, number of branches and/or holes [15] as well as moments, projections, distributions, graphometrics, directions, curvatures and chain codes [16]. Local features were also employed for offline ASV with notable results [17-32]. In recent years, we witnessed a shift of ASV research from the classic approaches towards the more data driven machine

learning t ones. These methods typically exploit spatial associations of raw pixels, or properties of them, that are part of the static signature image trace. Characteristic examples of the above aforementioned family include among others Bag of Words (BoW) or Histogram of Templates [33-36] compact correlated features of histogram oriented gradients [37], sparse representation [38-40 and last but not least early attempts [41-42] or recently published Deep Learning oriented approaches [15-16], [43-49].

It has also been reported that SV can utilize structural pattern recognition approaches using graphs, which is considered a powerful representation formalism [16]. In the literature one may find a limited number of research efforts which study graphs for offline SV [50-53]. The graph edit distance has been recently proposed for SV by combining the complementary strength of structural and statistical signature models in a multiple classifier system [54]. In [16], the authors updated the graph edit distance with the addition of a network architecture named DenseNEt-121 in order to allow features from lower layers to be propagated directly to the higher layers of the network. Results have been derived on a number of popular datasets like CEDAR [55], UTSIG [56], GPDS Synthetic [57] and MCYT-75 [58].

Quite recently, image visibility graphs (IVG) have been introduced as a way to map scalar fields and subsequent grayscale or colored images into graphs [59], [60]. Throughout the early literature, VGs have been proposed for building the bridge between time series analysis and network science. VGs model the underlying dynamics of a given time series by mapping its structure into an accompanying graph. More specific, natural as well as horizontal visibility graphs (VG/HVGs) were proposed as an assembly of mappings between ordered sequences and graphs, in order to perform graph theoretical time series analysis. Therefore, VGs can be viewed as a tool for mining data derived from a graph. VGs have been found applicable to a number of situations; to name a few domains we report physics [61] and economics [62]. Graphs, as well as their corresponding VGs can be represented with a number of graph features, global or local, which in turn can be evaluated and utilized for problems associated for description and classification purposes. In addition, visibility graphs are a parameter free mining technique so it can be easy to use and yield reproducible results.

In this work, inspired by the recent use of image visibility graphs for mapping images into networks, we introduce for the first time their use in offline SV literature. Specifically, we propose a novel feature extraction method for offline SV by exploring global and local properties of visibility graphs. Following are the characteristics of the proposed approach:

1. We employ two types of visibility graphs namely natural IVG as well as horizontal IHVG. Hence, IVG/IHVG graphs are created from any signature image by considering pixels as nodes and linking all nodes that satisfy a number of visibility criteria in specific direction, i.e. rows, columns, and diagonals.

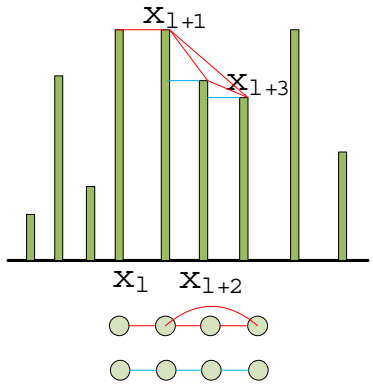

Figure 1: Example of the natural (red) and the horizontal (blue) visibility criterion applied to a set of time data points. For simplicity, the search window has been set to four in order to depict also a subgraph of order four (i.e. a motif).

2. We measure global properties of the VGs which unfold topological information of the entire graph. Specifically, we employ global graph-based image analysis by examining the degree distribution of the graph as a simple unsupervised universal feature extractor.

3. We also apply localized feature extraction by introducing and exploring sequential natural or horizontal visibility-graph motifs profiles, defined as smaller substructures of n consecutive nodes that appear with characteristic frequencies. The specific visibility motifs which will be used in this work are of low order (in our case four) and provide a mapping into a six-dimensional feature vector that has been found to be computationally efficient (we merely count the presence of six simple inequalities which is computationally tractable) as well as highly informative [63], [64]. In summary, local information is derived from local patches of signature images by a) coding according to the sequential natural or horizontal visibility-graph motifs and b) proper pooling the corresponding codes in order to create features. In all cases, a spatial equimass pyramid scheme inflates the basic feature extraction method into a higher dimensional one which finally feeds the verification stage.

The rest of the paper is organized as follows. Section 2 presents the basic postulates for the visibility graphs as well as the sequential visibility motifs. Section 3 describes the system's architecture, and provides the proposed feature extraction method. Section 4 reports the experimental methods and results. Finally, section 5 provides the conclusion.

2. Visibility graphs and motifs

Let us consider an ordered sequence $\{\mathbf{x}_t\}_{t=1}^{N}$ such that:

$\mathbf{x}_t \in \mathbb{R}^m$, $m \geq 1$. For *m*=1, this real valued series of N consecutive data points may be used as basis for modelling the output of a simple or complex dynamic process. We provide the following definitions for two types of VGs which are extracted from the $\{x_t\}_{t=1}^{N}$ sequence [59].

Definition: *A natural VG is an undirected graph of n nodes, where each node i is labelled according to the time order of its corresponding datum* x_i. *That is,* x_1 *is mapped into node i=1,* x_2 *into node i=2, and so on. Then, two nodes labeled i and j (we are also assuming that i < j without loss of generality) are said to be connected by an (undirected) link if and only if* x_i *and* x_j *share a type of "line-of-sight" edge E. That is, one can draw an edge E for connecting nodes i, j that does not intersect any intermediate datum* x_k, *with* $i < k < j$. *Concluding, nodes i, j are said to be connected is the following visibility (or convexity) criterion is satisfied:*

$$x_k < x_i + \frac{k-i}{j-i}\left[x_j - x_i\right],\ \forall k : i < k < j \qquad (1)$$

In a similar way, the HVG is defined by a similar definition. In this case however, we use a horizontally connecting edge *E* for nodes *i, j*, that does not intersect any other intermediate datum x_k. Thus, for HVG the following criterion, which is a ordering one, must be satisfied: $x_k < \inf(x_i, x_j),\ \forall k : i < k < j$. Figure 1 depicts graphically the aforementioned VG/HVG definitions with an additional constrain of the length of the signal (window size) equal to four. Following, we now extent the above formulations to images [60]:

Definition: *Let* $I = \{I(i,j)\} \in \mathbb{R}^{N \times N}, I(i,j) \in \mathbb{R}$ *be an image. The IVG is a graph of* N^2 *nodes where each node is labelled by the indices of its corresponding datum* $I(i,j)$ *such that two nodes i,j and i',j' are connected by a line of sight edge E if the following criterions are satisfied for some integer p:*

$$(i = i') \vee (j = j') \vee \left[(i = i' + p) \wedge (j = j' + p)\right] \qquad (2)$$

and $I(i,j)$, $I(i',j')$ *are connected in the VG defined over the ordered sequence which includes i,j and i',j'.*

In a similar way, the IHVG holds if we replace the VG criterion with the HVG one. To conclude, we will now provide the definitions for the natural and horizontal sequential visibility motifs.

Definition: *Let us consider a VG or a HVG of N nodes, related to a sequence of N data points. Set n < N and let us conceive an entity with the following elements: a) all the sequential subgraphs formed by the sequence of nodes* $\{s, s+1, ..., s+n-1\}$, $s \in [1, ...N-n+1]$ *(as depicted also in figure 1 for the case n=4) and b) the lines-edges from the VG or HVG of the subgraph that connects only these nodes. These entities are defined to be the sequential n-node motifs of the VG or HVG.*

In other words, we extend the definition of visibility to handle two-dimensional signal (image patches) by simply extending the visibility criteria along one-dimensional sections of the signal (scanning horizontal, vertical and diagonal directions). Now, let Φ_m to be the frequency of appearance of a specific *n*-node motif *m*, and therefore define $Z^n = (\Phi_1^n, ..., \Phi_{M_n}^n)$ to be the overall *n*-motif profile. This can be viewed as a discrete probability distribution with $\left\|Z^n\right\|_1 = 1$ and the number of degrees of freedom equal to $M_n - 1$. Henceforth, we will use for the motif size the value of *n* = 4 since it has been demonstrated that motifs of that order are, on the one the simplest non-trivial to be

TABLE 1: SET OF HVG AND VG MOTIF RELATIONS BETWEEN FOUR ARBITRARY CONSECUTIVE POINTS [x_0, x_1, x_2, x_3]

Label	motif	Inequality Set
HVG 1		$(\forall(x_0,x_1), x_2 < x_1 \wedge x_3 < x_2) \vee (\forall(x_0,x_3), x_1 > x_0 \wedge x_2 > x_1)$
HVG 2		$\forall x_0, x_1 < x_0 \wedge x_2 = x_1 \wedge x_3 > x_2$
HVG 3		$(\forall x_0, x_1 < x_0 \wedge x_1 < x_2 < x_0 \wedge x_3 < x_2) \vee (\forall x_0, x_3), x_1 < x_0 \wedge x_2 > x_0$
HVG 4		$(\forall x_0, x_1 > x_0 \wedge x_2 < x_1 \wedge x_3 > x_2) \vee (\forall x_0, x_1 < x_0 \wedge x_2 < x_1 \wedge x_2 < x_3 < x_1)$
HVG 5		$\forall x_0, x_1 < x_0 \wedge x_1 < x_2 < x_0 \wedge x_3 > x_2$
HVG 6		$\forall x_0, x_1 < x_0 \wedge x_2 < x_1 \wedge x_3 > x_1$
VG 1		$(\forall x_0, x_1),\ x_2 < 2x_1 - x_0 \wedge x_3 < 2x_2 - x_1$
VG 2		$(\forall x_0, x_1),\ x_2 > 2x_1 - x_0 \wedge x_3 < 1.5x_2 - 0.5x_0$
VG 3		$(\forall x_0, x_1),\ x_2 < 2x_1 - x_0 \wedge 2x_2 - x_1 < x_3 < 3x_1 - 2x_0$
VG 4		$(\forall x_0, x_1),\ x_2 > 2x_1 - x_0 \wedge 1.5x_2 - 0.5x_0 < x_3 < 2x_2 - x_1$
VG 5	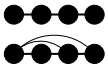	$(\forall x_0, x_1),\ x_2 < 2x_1 - x_0 \wedge x_3 > 3x_1 - 2x_0$
VG 6	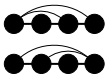	$(\forall x_0, x_1),\ x_2 > 2x_1 - x_0 \wedge x_3 > 2x_2 - x_1$

considered and on the other, they are highly informative [63].

In theory, VG/HVG motifs are evaluated in linear time by exploring the sequence $\{x_n\}$ with the aid of a set of inequalities. For example for a 4-point sequence $x=[x_0, x_1, x_2, x_3]$ with $n=4$, $x \in [-\infty, \infty]$, that fulfils the Markov property: $f(x_l | x_{l-1}, x_{l-2}, ...) = f(x_l | x_{l-1})$ the HVG motif Φ_1^4 is defined as:

$$\Phi_1^4 = \int_{-\infty}^{\infty} f(x_0)dx_0 \int_{-\infty}^{\infty} f(x_1|x_0)dx_1 \int_{-\infty}^{x_1} f(x_2|x_1)dx_2 \times \int_{-\infty}^{x_2} f(x_3|x_2)dx_3 + \int_{-\infty}^{\infty} f(x_0)dx_0 \int_{x_0}^{\infty} f(x_1|x_0)dx_1 \times \int_{x_1}^{\infty} f(x_2|x_1)dx_2 \int_{-\infty}^{\infty} f(x_3|x_2)dx_3 \quad (3)$$

In a similar way, the natural VG profile for a case similar to the aforementioned one is also defined as:

$$\Phi_1^4 = \int_{-\infty}^{\infty} f(x_0)dx_0 \int_{-\infty}^{\infty} f(x_1|x_0)dx_1 \int_{-\infty}^{2x_1-x_0} f(x_2|x_1)dx_2 \times \int_{-\infty}^{2x_2-x_1} f(x_3|x_2)dx_3 \quad (4)$$

In both eqs. (3), (4) the range for each integral is implicitly provided by the inequality sets portrayed in Table 1 for the HVG and VG respectively. It needs to be pointed out here that for the VG case of Table 1, there are two additional theoretical motifs; however their inequality set is the empty set, making the admissible motif size equal to six. Similar to the VG case, motif HVG2 is admissible only when the data series take values from a finite set, in order to have a finite probability [64]. Given the fact that we are coping with digital gray-scale images which are defined over a finite set of values, we will keep this specific motif. The integrals of eqs. (3), (4) seem tricky and sometimes their calculation can be made only with arithmetic methods. However in our case, which utilizes discrete valued data points (the pixel values) the sequential *n*-node motifs VG or HVG are evaluated by simply detecting the existence of the inequalities of Table 1. This is repeated by sequentially sliding a one dimensional window of size *n* inside the graph space which finally leads to the evaluation of the $Z^4 = (\Phi_1^4, ..., \Phi_6^4)$ profiles.

Given the short nature of the sequential VG/HVG graph motifs, it seems challenging to transfer these concepts from time series to local patches of signature images in order to encode any visibility relation between the signature pixels. Signatures are not natural images; they have a sparse spatial nature and neighboring pixels usually share a high degree of correlation. Thus, local signatures patches of relative small size, e.g. five should be taken into account since it determines the dimensionality and shape of any underlying local manifolds. Theoretically, if the patch size grows then a more complex manifold shall have to be taken into account since curved edges may appear within the patches, which in turn will require extra degrees of freedom to be included to the signal's model. The nature of the signal within signature patches is such that can be modeled with few only parameters, if the patch size is small-enough, something that indicates a low-dimensional underlying manifold structure [38]. Small sized patches contain signals (i.e. pixel values) that resemble the ones that sequential VGs/HVGs motifs can characterize. In this work, the term "sequential" is related to the way that the visibility operation is applied to the signature image.

3. System architecture

This section serves as a bridge between the VG/HVG concepts and their application to the SV domain. Quantification of graph's meaningful properties can be realized in two diverse ways: a) globally, which measures topological information on the entire image- graph and b) locally which accounts for properties of patches defined as small subregions of pixels.

3.1. Global features

Graphs can be associated with a number of topological properties of their nodes. Therefore, one can quantify a mapping of these properties to countable features by labeling the nodes of an image according to a specific property of its IVG/IHVG. Thus, a feature matrix which

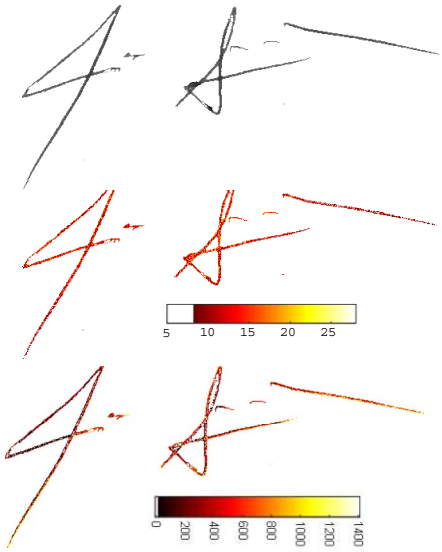

Figure 2: Example of a two-dimensional *degree* IVG plots for a signature image. The upper part is the original signature image while the lower parts represent the corresponding IHVG/IVG degree plots. Colored legends represent the degree of a node.

reflects the spatial relations of the associated signature pixels can be constructed and subsequently coded. In our case, the *degree* matrix or plot D_{IVG} or D_{IHVG}, defined for each individual matrix datum $D(i,j)$ as, the number of edges that are incident to its nodes (ij), has been selected. The *degree* matrix can be regarded to be a two-dimensional extension of the *degree* sequence which is defined as the set of the degree of a node associated to this specific datum. This is due to the fact that it has been found to be an informative global property, given the fact that HVGs are in bijection to their degree sequence [60], [65]. The resulted global feature vector for each signature image is its corresponding *degree* distribution *P(k),* defined as the percentage of pixels that have degree *k*. Figure 2 presents graphically the two-dimensional *degree* plot of a signature image for the case of IHVG/IVG. Concluding, for each signature image a *degree* plot is derived for the IVG and the IHVG. Prior to the feature formation a number of technical details must be reported. First, the *degree* of the background pixels of the image is up to 8 (3 and 5 for the corners and borderlines) for the HVG case and up to 19 for the VG case. Thus one can drop out these values in order to create the *P(k) degree* distribution. Second, it is expected that different images may exhibit different *max(k)* value due to their natural variability. However, experiments have demonstrated that for the case of IHVG, a number of *max(k)*=25 covers almost the 95-99% of the signature trace pixels. Consequently, we truncated for any signature image its initial *P(k)* distribution, to a corrected one *P(k')* with 17 indexes: $k'=[9,\ldots,25]$. For the case of IVG, due to its relaxed visibility criterion, the initial *P(k')* distribution indexes range is $k'=[20,\ldots,1550]$ and in addition, histogram bins have been restructured to a total of 100 new equal-spaced bins, that is: $k'=[k'_1,k'_2,\ldots,k'_{100}]$: $k'_1=\{20,\ldots 35\}$, $k'_2=\{36,\ldots 50\}$, $k'_{100}=\{1534,\ldots,1550\}$.

3.2. Local features

In a direct analogy to several contemporary machine learning techniques, local information is also explored by means of signature patch extraction and processing. As already mentioned, the offline handwritten signature forms a special type of two dimensional scalar field which exhibits a degenerate structure. Therefore it is anticipated that signals of this kind and subsequently their graphs, shall lie on a low dimensional subspace. So, it makes sense to mask the signature trace pixels, and employ local patch extraction. The basic patch size was set to five (i.e. a 5x5 pixel window) although experiments have been also carried out with patches having size equal to 7, 9, 11 and 13. For each signature patch VG/HVG sequential visibility motifs of size four were evaluated for each line, column, main and secondary diagonal. In addition, the patch window was further explored by converting the two-dimensional image patch to a one-dimensional signal by sequential

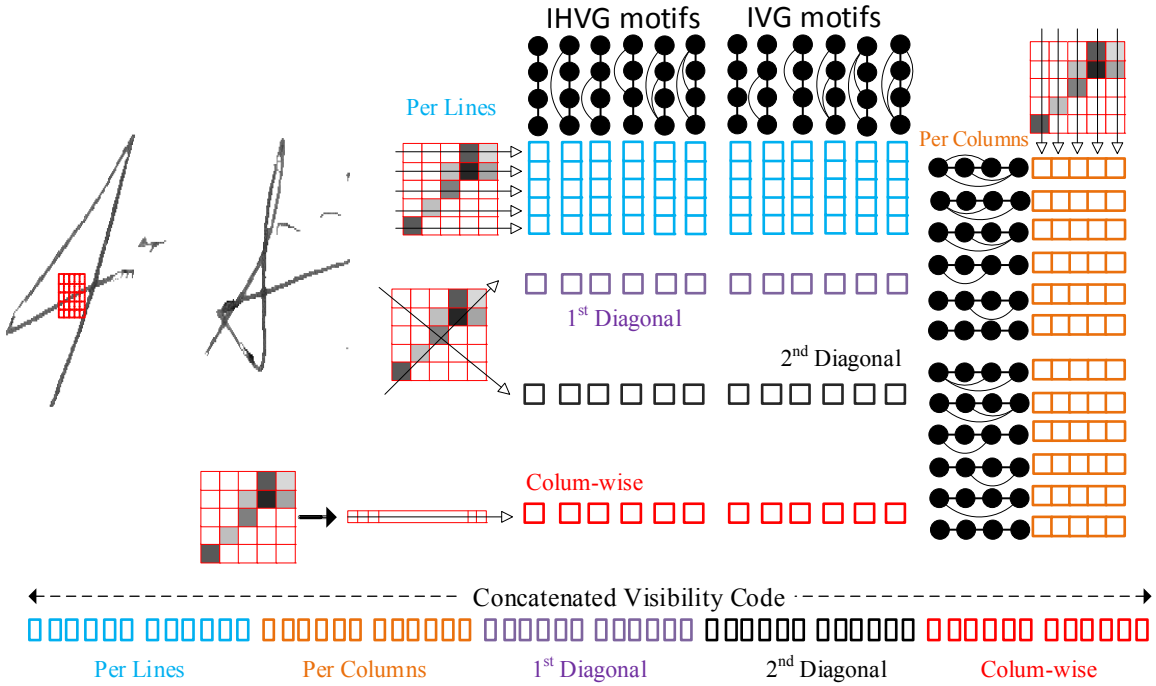

Figure 3: Example of a local visibility code with sequential motifs of size four. Left, image with a selected local patch of size five. Right, local IVG/IHVG motif coding for each line, column main and secondary diagonal, as well as a column-wise patch vector. Down, the final concatenated local sequential visibility code C.

column-wise concatenation. Given the fact that each VG/HVG of size four generates a six-dimensional feature vector, it is easy to conceive that any signature patch $p_i \in \mathbb{R}^{patchsize \times patchsize}$ is transformed to a resulted $c_i \in \mathbb{R}^{60}$ visibility code. Figure 3 depicts graphically the visibility coding for an arbitrary selected patch of a signature trace. We locate signature pixels, take small subregions (i.e. patches) around them and for each patch, count the number of motif's appearance in a) row as well as column rasterized format, b) diagonal rasterized format and c) a column-wise, vectored format. Following the creation of the visibility code matrix $C \in \mathbb{R}^{60 \times (\#sig\_trace\_pixels)}$ for a signature trace, three signature descriptors are formed as the outcome of three predefined types of pooling namely the average $F_{AV}(C)$, max $F_{MAX}(C)$ and the standard deviation $F_{STD}(C)$ defined as:

$$F_{AV}(C) = \{\forall j, f_j^{F_{AV}}\} = \{\frac{1}{\#\,pixels} \sum_{i=1}^{\#\,pixels} c_i[j]\} \quad (5)$$

$$F_{\infty}(\mathrm{C}) = \{\forall\, \mathrm{j}, f_j^{F_{\infty}} \triangleq \max\left|c_i[\mathrm{j}]\right|\} \quad (6)$$

$$F_{STD}(\mathrm{C}) = \{\forall j, f_j^{F_{STD}}\} = \{\sqrt{\frac{\sum_{i=1}^{\#\,pixels} (\mathrm{c}_i[\mathrm{j}] - f_j^{F_{AV}})^2}{\#\,pixels - 1}}\} \quad (7)$$

with *j=1:60*. Additional growth of the feature vector is realized by applying the above described pooling strategies to patches of image segments formed by specially designed equimass spatial pyramids.

4. Experiments

4.1. Datasets

Two popular signature datasets were used in order to demonstrate the effectiveness of the proposed system. The first one was created at CEDAR, Buffalo University [55]. For each one of the 55 total enrolled signatories, a total of forty-eight signature specimens (24 genuine and 24 simulated) confined in a 50 mm by 50 mm square box were provided and digitized at 300 dpi. The simulated signatures found in the CEDAR database are composed from a mixture of random, simple and skilled forgeries. The second signature database used was the off-line version of the MCYT-75 signature database [58]. A total of 15 genuine and 15 simulated signature samples were recorded for each one of the 75 enrolled writers at a resolution of 600 dpi. The preprocessing stage comprises of thresholding (Otsu's method) and morphological thinning. The resulted gray level image is formed by taking into account the gray level pixels of the original image masked at the locations returned by the thinning operation [38]. Due to the dissimilar acquisition settings, and especially the acquisition resolution of the two signature datasets, the thinning levels for the CEDAR, MCYT datasets have been set to one and two correspondingly. In addition, for the sake of simplicity we report results when the number of equimass segments has been set to four (2×2) and sixteen (4×4) for the CEDAR and MCYT-75 datasets [38].

4.2. Methods

We follow a writer dependent SV approach. That is a dedicated model is being built for every signatory in a dataset. For both global and local feature extraction cases, the number of genuine reference samples for each writer N_{GEN}^{REF} has been set to ten, in order to comply with the number used by the most popular experimental setups in offline SV for creating the positive class $\omega^{\oplus}$. In a similar way, a population of $N_{RF} = 30$ random forgeries (selected as random genuine samples from other signatories) creates the corresponding negative class ω^{-} , thus creating the learning set LS= $\{\omega^{\oplus}, \omega^{-}\}$.

According to the aforementioned discussion cited in paragraph 3.1, for the case of global features the HVG method creates for each image, a 17-dimensional feature vector HV while the corresponding natural VG method creates a 100-dimensional NV feature. Thus, for the LS we have, for the $\omega^{\oplus}$ and ω^{-} classes: $HV \in \mathbb{R}^{10 \times [17 \times (\#segments+1)]}$, $NV \in \mathbb{R}^{30 \times [100 \times (\#segments+1)]}$ respectively. For the case of local sequential motif features and any associative pooled sequential visibility feature vector (SVV), the reference $SVV_{REF} \in \mathbb{R}^{10 \times [60 \times (\#segments+1)]}$ is been created to account for the genuine class while in a similar way, the random forgery visibility vector $SVV_{RF} \in \mathbb{R}^{30 \times [60 \times (\#segments+1)]}$ represents the

TABLE 2. VERIFICATION ERROR RATES (%) FOR THE CEDAR AND MCYT-75 SIGNATURE DATASETS. GLOBAL APPROACH. HV, NV FEATURES

Type of *degree* plot	CEDAR: 1 entire image & 4 segms.				MCYT75: 1 entire image & 16 segms.			
	Hard Decision		EER(S)	$P_{FAR(R)}$	Hard Decision		EER(S)	$P_{FAR(R)}$
	$P_{FAR(S)}$	P_{FRR}	user_thresh	@EER(S)	$P_{FAR(S)}$	P_{FRR}	user_thresh	@EER(S)
Horizontal Visibility	10.4	7.57	7.89	1.25	14.3	10.8	12.5	2.01
Natural Visibility	20.8	18.7	18.6	3.89	25.5	21.2	23.3	3.54

negative class.

In brief, for both global and local cases the LS is used as an input to a binary, radial basis SVM classifier. A holdout cross-validation procedure returns the optimum operational parameters for the SVM margin and scale with respect to the maximum value of the Area under Curve (AUC). Moreover, the cross-validation procedure provides for each writer the scores conditioned on the positive only $\omega^{\oplus}$ class samples $CVS^{\oplus}$. The testing stage makes use of questioned (designated as: Q) samples that originate from: the remaining genuine signatures (14 for CEDAR, 5 for MCYT), the skilled forgeries (S: 24 for CEDAR and 15 for MCYT) and a number of 44 or 64 random forgeries (R) by taking one random sample from the remaining writers which does not participate to the formation of the learning set. Results are reported by means of the well-known receiver operating characteristic (ROC) probabilities: the $p_{FAR(S)}$ and p_{FRR} error rates are computed as a function of a sliding threshold, whose extremes lie between the minimum and maximum values of the $CVS^{\oplus}$ cross validation procedure.

Two different verification approaches are reported. In the first, a hard threshold is utilized to separate the genuine sample from skilled forgeries. This selection relies only on the $\omega^{\oplus}$ genuine reference samples as they are the only ones available for learning. In a typical scenario, this hard threshold is set to 50% of the average value of $\omega^{\oplus}$ scores. Additionally, we report also a popular metric which is the equal error rate per user threshold: $EER(S)_{\text{user-threshold}}$ to be defined as the point in which $p_{FAR(S)} = p_{FRR}$. The experiments were repeated ten times and their average values are reported. In addition, at this specific EER(S) we evaluate the random forgery-(R) $p_{FAR(R)}$ error rate by using the genuine samples of the remaining writers of the testing set.

TABLE 4. ERROR RATES (EER(S) %) FOR THE CEDAR AND MCYT-75 SIGNATURE DATASETS. VARIABLE PATCH SIZE. LOCAL APPROACH. SVV FEATURES

Patch Size	CEDAR Av. & Std (SVV)	MCYT75 Av. & Std (SVV)	CEDAR Average (SVV)	MCYT75 Average (SVV)
5	0.04	1.61	0.05	1.54
7	0.05	1.67	0.06	1.80
9	0.08	2.32	0.09	2.47
11	1.02	2.75	1.05	2.93
13	1.03	3.12	1.05	3.42

4.3. Results

Tables 2, 3 present the verification results obtained when the aforementioned experimental protocols were performed. In order to maintain the uniformity of results with table 2, table 3 presents also the verification error rates when the $SVV_{REF,RF\ or\ Q}$ vectors are partitioned in halves into their horizontal/natural parts $SVV^{\{H\ or\ N\}}_{REF,RF\ or\ Q}$. Inspection of Tables 2, 3 shows emphatically that the local approach which employs sequential motifs surpasses the global oriented one as expressed by its degree distribution. For the problem of offline signature verification, this seems to be a reasonable assumption as it has already been reported that local features based systems outperform global ones in terms of error rates [18]. However, we feel that a number of other measures like density, K-kore, assortativity [66], should be studied also in future research activities.

In order to examine the effect of the patch size in the verification error, we performed a number of experiments with increasing patch size. Table 4 shows clearly that, the verification error increases when the patch size also increases. The results seem to be in accordance with the discussion provided in section 2, where a higher order patch will lead to a more complex manifold which in turn will require extra degrees of freedom to be included to the signal's model. Nevertheless, although higher order patches seem to provide weaker verification results, we feel that we

TABLE 3. VERIFICATION ERROR RATES (%) FOR THE CEDAR AND MCYT-75 SIGNATURE DATASETS. LOCAL APPROACH. SVV FEATURES

Pooling method	CEDAR: 1 entire image & 4 segments				MCYT75: 1 entire image & 16 segments			
	Hard Decision		EER(S)	$P_{FAR(R)}$	Hard Decision		EER(S)	$P_{FAR(R)}$
	$P_{FAR(S)}$	P_{FRR}	user_thresh	@EER(S)	$P_{FAR(S)}$	P_{FRR}	user_thresh	@EER(S)
Average (SVV^H)	1.23	0.97	0.30	0.00	4.37	5.32	1.59	0.02
Max (SVV^H)	25.8	23.6	22.2	2.93	11.5	23.2	16.2	2.31
Std (SVV^H)	4.69	4.18	2.72	0.04	6.20	7.18	2.40	0.02
Average (SVV^N)	2.89	2.14	1.01	0.02	6.00	6.95	2.03	0.02
Max (SVV^N)	21.1	19.8	19.4	2.15	16.7	13.9	13.8	2.19
Std (SVV^N)	4.53	4.02	2.01	0.03	8.61	8.09	2.81	0.03
Average (SVV)	1.28	1.06	0.51	0.00	4.37	5.21	1.54	0.01
Max (SVV)	19.4	18.2	17.0	1.83	15.7	12.6	12.55	2.54
Std (SVV)	4.55	4.13	1.99	0.04	6.22	7.29	2.42	0.03
Av. & Std (SVV)	1.25	0.99	0.41	0.00	4.38	5.32	1.61	0.02

will have to examine sequential motifs of larger size (e.g. five) in order to be able to provide a more comprehensive opinion. This is in accordance with the fact that motifs of order four have only 5 independent degrees of freedom Note however, that this is beyond the scope of this work.

Table 5 presents a summary of results for the CEDAR and MCYT-75 signature datasets, with other approaches found on the literature. For completeness, we summarize results derived from writer independent (WI) approaches. It must be kept in mind that attaining a fair comparison between these results can be a very difficult task, because there are a number of factors that affect it during the classifier construction and evaluation [16-17], [34]. We summarizing results having in mind either the Average or the Equal Error Rates (AER/EER) for the skilled forgeries (S) case. Therefore we feel that the proposed method achieves a low error of verification which is considered to be at least comparable to the ones derived from state of the art methods.

5. Conclusions

In this work a novel, parameter free, candidate graph mining method for offline signature coding and verification has been introduced. It proposes the use of visibility graphs extracted from raw signature trace pixels of a grayscale image for coding and verification purposes. This is the first time in the literature were visibility graphs have been agnostically used in order to map the signature pixels into an unordered representation in both global and local scenarios. Considering the global scenario, we employ graph-based image analysis by examining the degree distribution of the nodes of a graph as a simple unsupervised universal feature extractor. Local information has been derived by proposing a novel feature extraction method which relies on the calculation of the probability distributions-or profiles- of small subgraphs (or motifs) of order four. Motif profiles intuitively convert local patches of signature images into sequential natural and/or horizontal visibility codes. A number of pooling functions operate on the motif codes in a spatial pyramid context in order to create the final feature vector. After evaluating our approach with two popular signature datasets and summarizing with related research efforts, we can assert that competent performance can be obtained following this model. We plan to expand this work as follows: First we plan to explore other graph oriented descriptions and statistics to derive global information. Second, we plan to investigate the use of higher order sequential motifs; in this case we need to keep in mind that the number of motifs increases exponentially with motif size. Third, we expect to include several other signature datasets with variable design constraints like number and size of bounding boxes, natural or synthetic samples, in order to simulate actual working conditions.

TABLE 5. SUMMARY OF RESULTS (**WD**, **WI**) FOR CEDAR & MCYT75. RESULTS ON AER OR EER BASIS % (S).

Method	**# Ref.**	**AER / EER**
CEDAR		
Morphology (**WI**) [67]	1	11.6
Surroundness (**WI**) [25]	1	8.33
Chord moments [68]	16	6.02
Gradient & concavity [69]	16	7.90
Zernike moments [69]	16	16.4
G. S & C (**WI**) [55]	16	21.9
Partially Ordered Sets [30]	5	4.12
Curvelet (**WI**) [70	12	5.60
Gradient LBP + LRF [27]	16	3.52
SigNet / SigNet-F [47]	12	4.63
SigNet-SPP-300dpi [46]	10	3.60
SigNet-SPP-300dpi (fine tun.) [46]		2.33
Chain code [71]	12	7.84
B.O.W with KAZE [72]	16	1.60
V.L.A.D with KAZE [33]	16	1.00
Gradient Direction [73]	14	6.01
Pattern Spectrum [74]	16	9.58
Co. Occurrence (**WI**) [29]	5	2.11
Archetypes [40]	5	2.07
Triplet Nets-Graph edit dist. [16]	10	5.91
Tree structured sparsity [39]	5	2.30
Compact Correlated [37]	N/A	0.00
Deep Sparse Coding [75]	5	2.82
Sparse Coding [38]	10	0.79
Inverse Network (**WI**) [15]	N/A	3.62
HOCCNN [49]	12	4.94
Proposed: Average (SVV)	**10**	**0.51**
MCYT-75		
L.B.P [23]	10	7.08
Triplet Nets-Graph Edit Dist. [16]	10	3.91
Partially Ordered Sets [30]	5	6.02
Contours [76]	10	6.44
Global and Local Slant [22]	10	9.28
Discrete Radon Transform [77]	10	9.87
HOG & Deep-MML [48]	10	9.86
SigNet / SigNet-F [47]	10	3.00
SigNet-SPP-300dpi [46]	10	3.60
SigNet-SPP-300dpi (fine tun.) [46]		2.33
H.O.T [35]	10	18.15
BoVW - VLAD - KAZE [33]	10	6.4
Archetypes [40]	5	3.97
Tree structured sparsity [39]	5	3.52
Sparse Coding [38]	10	1.37
HOCCNN [49]	10	5.46
Proposed: Average (SVV)	**10**	**1.54**

References

[1] C. Vielhauer, Behavioural Biometrics, Public Service Review, European Union, 2005.

[2] D. Impedovo and G. Pirlo, Automatic signature verification in the mobile cloud scenario: survey and way ahead, IEEE Transactions on Emerging Topics in Computing:1-15, 2018.

[3] R. Blanco-Gonzalo, O. Miguel-Hurtado, A. Mendaza-Ormaza, and R. Sanchez-Reillo, Handwritten signature recognition in mobile scenarios: Performance evaluation, IEEE International Carnahan Conference on Security Technology:174-179, 2012.

[4] N. Sae-Bae and N. Memon, Online Signature Verification on Mobile Devices, IEEE Transactions on Information Forensics and Security, (9):933-947, 2014.

[5] J. Galbally, M. Diaz-Cabrera, M. A. Ferrer, M. Gomez-Barrero, A. Morales, and J. Fierrez, On-line signature recognition through the combination of real dynamic data and synthetically generated static data, Pattern Recognition, 48:2921-2934,

[6] N. Sae-Bae, N. Memon, and P. Sooraksa, Distinctiveness, complexity, and repeatability of online signature templates, Pattern Recognition, 84:332-344, 2018.

[7] V. Venugopal and S. Sundaram, An improved online writer identification framework using codebook descriptors, Pattern Recognition, 78:318-330, 2018

[8] Moises Diaz, Miguel A. Ferrer, Donato Impedovo, Muhammad Imran Malik, Giuseppe Pirlo, and R. Plamondon., A Perspective Analysis of Handwritten Signature Technology, ACM Comput. Surv., 51(6):1-39, 2018.

[9] A. Morales, D. Morocho, J. Fierrez, and R. Vera-Rodriguez. Signature authentication based on human intervention: performance and complementarity with automatic systems. IET Biometrics 6(4):307-315, 2017.

[10] R. Plamondon and G. Lorette, Automatic signature verification and writer identification -- the state of the art, Pattern Recognition, 22:107-131, 1989.

[11] F. Leclerc and R. Plamondon, Automatic Signature Verification: The State Of The Art: 1989–1993, International Journal of Pattern Recognition and Artificial Intelligence, 8:643-660, 1994.

[12] R. Plamondon and S. N. Srihari, Online and off-line handwriting recognition: a comprehensive survey, IEEE Transactions on Pattern Analysis and Machine Intelligence, 22:63-84, 2000.

[13] D. Impedovo and G. Pirlo, Automatic Signature Verification: The State of the Art, IEEE Transactions on Systems, Man and Cybernetics, Part C: Applications and Reviews, 38:609-635, 2008.

[14] R. A. Huber and A. M. Headrick, Handwriting identification: facts and fundamentals. Boca Raton: CRC Press, 2010.

[15] P. Wei, H. Li, and P. Hu, Inverse Discriminative Networks for Handwritten Signature Verification, CVPR, 5764-5772, 2019.

[16] P. Maergner, V. Pondenkandath, M. Alberti, M. Liwicki, K. Riesen, R. Ingold, et al., Combining graph edit distance and triplet networks for offline signature verification, Pattern Recognition Letters, 125:527-533, 2019.

[17] E. N. Zois, A. Alexandridis, and G. Economou, Writer independent offline signature verification based on asymmetric pixel relations and unrelated training-testing datasets, Expert Systems with Applications, 125:14-32, 2019.

[18] M. I. Malik, M. Liwicki, and A. Dengel, Local features for off-line forensic signature verification, Advances in Digital Handwritten Signature Processing, World Scientific, 95-109, 2014.

[19] V. Nguyen, Y. Kawazoe, T. Wakabayashi, U. Pal, and M. Blumenstein, Performance Analysis of the Gradient Feature and the Modified Direction Feature for Off-line Signature Verification, ICFHR, 303-307, 2010.

[20] M. B. Yılmaz and B. Yanıkoğlu, Score level fusion of classifiers in off-line signature verification, Information Fusion, 32(B):109-119, 2016.

[21] R. Sabourin, G. Genest, and F. J. Preteux, Off-line signature verification by local granulometric size distributions, IEEE Transactions on Pattern Analysis and Machine Intelligence, 19:976-988, 1997.

[22] J. Fierrez-Aguilar, N. Alonso-Hermira, G. Moreno-Marquez, and J. Ortega-Garcia, An Off-line Signature Verification System Based on Fusion of Local and Global Information, in Biometric Authentication. 3087:295-306, 2004.

[23] J. F. Vargas, M. A. Ferrer, C. M. Travieso, and J. B. Alonso, Off-line signature verification based on grey level information using texture features, Pattern Recognition, 44:375-385, 2011.

[24] L. Batista, E. Granger, and R. Sabourin, Dynamic selection of generative–discriminative ensembles for off-line signature verification, Pattern Recognition, 45:1326-1340, 2012.

[25] R. Kumar, J. D. Sharma, and B. Chanda, Writer-independent off-line signature verification using surroundedness feature, Pattern Recognition Letters, 33:301-308, 2012.

[26] G. Pirlo and D. Impedovo, Verification of Static Signatures by Optical Flow Analysis, IEEE Transactions on Human-Machine Systems, 43:499-505, 2013.

[27] Y. Serdouk, H. Nemmour, and Y. Chibani, New off-line Handwritten Signature Verification method based on Artificial Immune Recognition System, Expert Systems with Applications, 51:186-194, 2016.

[28] M. A. Ferrer, J. F. Vargas, A. Morales, and A. Ordonez, Robustness of Offline Signature Verification Based on Gray Level Features, IEEE Transactions on Information Forensics and Security, 7:966-977, 2012.

[29] A. Hamadene and Y. Chibani, One-Class Writer-Independent Offline Signature Verification Using Feature Dissimilarity Thresholding, IEEE Transactions on Information Forensics and Security, 11:1226-1238, 2016.

[30] E. N. Zois, L. Alewijnse, and G. Economou, Offline signature verification and quality characterization using poset-oriented grid features, Pattern Recognition, 54:162-177, 2016.

[31] W. Bouamra, C. Djeddi, B. Nini, M. Diaz, and I. Siddiqi, Towards the design of an offline signature verifier based on a small number of genuine samples for training, Expert Systems with Applications, 107:182-195, 2018.

[32] S. Pal, A. Alaei, U. Pal, and M. Blumenstein, Performance of an Off-Line Signature Verification Method Based on Texture Features on a Large Indic-Script Signature Dataset, IAPR Workshop on Document Analysis Systems, 72-77, 2016.

[33] M. Okawa, From BoVW to VLAD with KAZE features: Offline signature verification considering cognitive

processes of forensic experts, Pattern Recognition Letters, 113:75-82, 2018.
[34] M. Okawa, Synergy of foreground–background images for feature extraction: Offline signature verification using Fisher vector with fused KAZE features, Pattern Recognition, 79:480-489, 2018.
[35] Y. Serdouk, H. Nemmour, and Y. Chibani, Handwritten signature verification using the quad-tree histogram of templates and a Support Vector-based artificial immune classification, Image and Vision Computing, 66:26-35, 2017.
[36] S.-J. Zhang, M. Y. Aysa, and K. Ubul, BoVW Based Feature Selection for Uyghur Offline Signature Verification, Chinese Conference on Biometric Recognition, 700-708, 2018.
[37] A. Dutta, U. Pal, and J. Lladós, Compact correlated features for writer independent signature verification, International Conference on Pattern Recognition, 3422-3427, 2016.
[38] E. N. Zois, D. Tsourounis, I. Theodorakopoulos, A. L. Kesidis, and G. Economou, A Comprehensive Study of Sparse Representation Techniques for Offline Signature Verification, IEEE Trans. on Biometrics, Behavior, and Identity Science, 1:68-81, 2019.
[39] E. N. Zois, M. Papaggianopoulou, D. Tsourounis, and G. Economou, Hierarchical Dictionary Learning and Sparse Coding for Static Signature Verification, IEEE Conference on Computer Vision and Pattern Recognition Workshops, 432-442 , 2018.
[40] E. N. Zois, I. Theodorakopoulos, and G. Economou, Offline Handwritten Signature Modeling and Verification Based on Archetypal Analysis, IEEE International Conference on Computer Vision, 5514-5523, 2017.
[41] B. Ribeiro, I. Gonçalves, S. Santos, and A. Kovacec, Deep Learning Networks for Off-Line Handwritten Signature Recognition, 16th Iberoamerican Congress conference on Progress in Pattern Recognition, Image Analysis, Computer Vision, and Applications, 523-532, 2011.
[42] Khalajzadeh Hurieh, M. Mansouri, and M. Teshnehlab, Persian Signature Verification using Convolutional Neural Networks, International Journal of Engineering Research and Technology 1:7-12, 2012.
[43] M. B. Yılmaz and K. Öztürk, Recurrent Binary Patterns and CNNs for Offline Signature Verification, Proceedings of the Future Technologies Conference, Cham, 417-434, 2019.
[44] S. Masoudnia, O. Mersa, B. N. Araabi, A.-H. Vahabie, M. A. Sadeghi, and M. N. Ahmadabadi, Multi-Representational Learning for Offline Signature Verification using Multi-Loss Snapshot Ensemble of CNNs, Expert Systems with Applications, 133:317-330, 2019.
[45] M. B. Yilmaz and K. Ozturk, Hybrid User-Independent and User-Dependent Offline Signature Verification With a Two-Channel CNN, IEEE Conference on Computer Vision and Pattern Recognition Workshops, 639-647, 2018.
[46] L. G. Hafemann, L. S. Oliveira, and R. Sabourin, Fixed-sized representation learning from offline handwritten signatures of different sizes, International Journal on Document Analysis and Recognition 21:219-232, 2018.
[47] L. G. Hafemann, R. Sabourin, and L. S. Oliveira, Learning features for offline handwritten signature verification using deep convolutional neural networks, Pattern Recognition, 70:163-176, 2017.
[48] A. Soleimani, B. N. Araabi, and K. Fouladi, Deep Multitask Metric Learning for Offline Signature Verification, Pattern Recognition Letters, 80:84-90, 2016.
[49] S. Shariatmadari, S. Emadi, and Y. Akbari, Patch-based offline signature verification using one-class hierarchical deep learning, International Journal on Document Analysis and Recognition, 22:375-385, 2019.
[50] A. Bansal, P. Nemmikanti, and P. Kumar, Offline Signature Verification Using Critical Region Matching, Second International Conference on Future Generation Communication and Networking Symposia, 115-120, 2008.
[51] T. Fotak, M. Bača, and P. Koruga, Handwritten signature identification using basic concepts of graph theory, WSEAS Transactions on Signal Processing, 7:117-129, 2011.
[52] K. Riesen and H. Bunke, Approximate graph edit distance computation by means of bipartite graph matching, Image and Vision Computing, 27:950-959, 2009.
[53] R. Sabourin, R. Plamondon, and L. Beaumier, Structural interpretation of handwritten signature images, International Journal of Pattern Recognition and Artificial Intelligence, 8:709-748, 1994.
[54] P. Maergner, V. Pondenkandath, M. Alberti, M. Liwicki, K. Riesen, R. Ingold, and A. Fischer, Offline Signature Verification by Combining Graph Edit Distance and Triplet Networks, International Workshops on Statistical Techniques in Pattern Recognition and Structural and Syntactic Pattern Recognition, Cham, 470-480 2018.
[55] M. K. Kalera, S. Srihari, and A. Xu, Offline signature verification and identification using distance statistics, International Journal of Pattern Recognition and Artificial Intelligence, 18:1339-1360.
[56] A. Soleimani, K. Fouladi, and B. N. Araabi, UTSig: A Persian offline signature dataset, IET Biometrics, 6:1-8, 2016.
[57] M. A. Ferrer, M. Diaz-Cabrera, and A. Morales, Static Signature Synthesis: A Neuromotor Inspired Approach for Biometrics, IEEE Transactions on Pattern Analysis and Machine Intelligence, 37:667-680, 2015.
[58] J. Ortega-Garcia, J. Fierrez-Aguilar, D. Simon, J. Gonzalez, M. Faundez-Zanuy, V. Espinosa, et al., MCYT baseline corpus: a bimodal biometric database, IEE Proceedings Vision, Image and Signal Processing, 150:395-401, 2003.
[59] J. Iacovacci and L. Lacasa, Visibility graphs for image processing, IEEE Transactions on Pattern Analysis and Machine Intelligence, 2019.
[60] L. Lacasa and J. Iacovacci, Visibility graphs of random scalar fields and spatial data, Physical Review E, 96:012318, 2017.
[61] P. Manshour, M. R. Rahimi Tabar, and J. Peinke, Fully developed turbulence in the view of horizontal visibility graphs, Journal of Statistical Mechanics: Theory and Experiment, P08031, 2015.
[62] M.-C. Qian, Z.-Q. Jiang, and W.-X. Zhou, Universal and nonuniversal allometric scaling behaviors in the visibility graphs of world stock market indices, Journal of Physics A: Mathematical and Theoretical, 43:335002, 2010.
[63] J. Iacovacci and L. Lacasa, Sequential visibility-graph motifs, Physical Review E, 93:042309, 2016.
[64] J. Iacovacci and L. Lacasa, Sequential motif profile of natural visibility graphs, Physical Review E, 94:052309, 2016.

[65] B. Luque and L. Lacasa, Canonical horizontal visibility graphs are uniquely determined by their degree sequence, The European Physical Journal Special Topics, 226:383-389, 2017.
[66] D. Li, J. Lin, T. F. D. A. Bissyande, J. Klein, and Y. Le Traon, Extracting Statistical Graph Features for Accurate and Efficient Time Series Classification, International Conference on Extending Database Technology, 1-12, 2018.
[67] R. Kumar, L. Kundu, B. Chanda, and J. D. Sharma, A writer-independent off-line signature verification system based on signature morphology, International Conference on Intelligent Interactive Technologies and Multimedia, 261-265, 2010.
[68] M. M. Kumar and N. B. Puhan, Off-line signature verification: upper and lower envelope shape analysis using chord moments, IET Biometrics, 3:347-354, 2014.
[69] S. Chen and S. Srihari, A New Off-line Signature Verification Method based on Graph, International Conference on Pattern Recognition, 1-4, 2006.
[70] Y. Guerbai, Y. Chibani, and B. Hadjadji, The effective use of the one-class SVM classifier for handwritten signature verification based on writer-independent parameters, Pattern Recognition, 48:103-113, 2015.
[71] R. K. Bharathi and B. H. Shekar, Off-line signature verification based on chain code histogram and Support Vector Machine, International Conference on Advances in Computing, Communications and Informatics, 2063-2068, 2013.
[72] M. Okawa, Offline Signature Verification Based on Bag-Of-Visual Words Model Using KAZE Features and Weighting Schemes, IEEE Conference on Computer Vision and Pattern Recognition Workshops, 184-190, 2016.
[73] G. Ganapathi and R. Nadarajan, A Fuzzy Hybrid Framework for Offline Signature Verification, 5th International Conference in Pattern Recognition and Machine Intelligence, 121-127, 2013.
[74] B. H. Shekar, R. K. Bharathi, and B. Pilar, Local Morphological Pattern Spectrum Based Approach for Off-line Signature Verification, 5th International Conference in Pattern Recognition and Machine Intelligence, 335-342, 2013.
[75] D. Tsourounis, I. Theodorakopoulos, E. N. Zois, G. Economou, and S. Fotopoulos, Handwritten Signature Verification via Deep Sparse Coding Architecture, IEEE 13th Image, Video, and Multidimensional Signal Processing Workshop, 1-5, 2018.
[76] A. Gilperez, F. Alonso-Fernandez, S. Pecharroman, J. Fierrez, and J. Ortega-Garcia, Off-line Signature Verification Using Contour Features, 11th International Conference on Frontiers in Handwriting Recognition, 1-6, 2008.
[77] S. Y. Ooi, A. B. J. Teoh, Y. H. Pang, and B. Y. Hiew, Image-based handwritten signature verification using hybrid methods of discrete Radon transform, principal component analysis and probabilistic neural network, Applied Soft Computing, 40:274-282, 2016.